

Quantum interference from sums over closed paths for electrons on a three-dimensional lattice in a magnetic field: total energy, magnetic moment, and orbital susceptibility

Yeong-Lieh Lin* and Franco Nori†

Department of Physics, The University of Michigan, Ann Arbor, Michigan 48109-1120

We study quantum interference effects due to electron motion on a three-dimensional cubic lattice in a *continuously-tunable* magnetic field \mathbf{B} of *arbitrary* orientation and magnitude. These effects arise from the interference between magnetic phase factors associated with different electron closed paths. The sums of these phase factors, called lattice path-integrals, are “many-loop” generalizations of the standard “one-loop” Aharonov-Bohm-type argument, where the electron wave function picks up a phase factor $e^{i\Phi}$ each time it travels around a closed loop enclosing a net flux Φ . Our lattice path integral calculation enables us to obtain various important physical quantities through several different methods. The spirit of our approach follows Feynman’s programme: to derive physical quantities in terms of “sums over paths”. From these lattice path-integrals we compute analytically, for several lengths of the electron path, the half-filled Fermi-sea ground-state energy, $E_T(\mathbf{B})$, of noninteracting spinless electrons in a cubic lattice. Our expressions for E_T are valid for any strength of the applied magnetic field in any direction. Moreover, we provide an explicit derivation for the absolute minimum energy of the flux state. For various field orientations, we also study the quantum interference patterns and $E_T(\mathbf{B})$ by exactly summing over $\sim 10^{29}$ closed paths in a cubic lattice, each one with its corresponding magnetic phase factor representing the net flux enclosed by each path. Furthermore, an expression for the total kinetic energy $E_T(\mathbf{B}, \nu)$ for any electron filling ν close to one half is obtained. We also study in detail two experimentally important quantities: the magnetic moment $M(\mathbf{B})$ and orbital susceptibility $\chi(\mathbf{B})$ at half-filling, as well as the zero-field susceptibility $\chi(\mu)$ as a function of the Fermi energy μ .

I. INTRODUCTION

The quantum behavior of noninteracting tight-binding electrons on a two-dimensional (2D) lattice immersed in a perpendicular magnetic field has attracted much attention due to its important role in diverse areas of physics. For instance, the problem is intimately related to the quantum Hall effect. During the past few years, the ground-state energy of this system has also been intensively investigated^{1–3} in connection with mean-field studies of the t - J and Hubbard models of high- T_c superconductors. At half-filling, the absolute minimum of the kinetic energy has a half flux quantum ($\Phi_0/2$) per plaquette—called the flux state. In addition, there are local minima at flux values equal to $\Phi_0/2m$ with $m > 1$.

More recently, several groups have paid attention to the three-dimensional (3D) case: the kinetic energy of a 3D noninteracting electron gas under the influence of both a strong periodic potential and a magnetic field. For instance, for several rational values of the magnetic field, Skudlarski and Vignale⁴ analyzed the changes in the ground-state properties induced by the addition of hopping in the direction parallel to the uniform magnetic field. Hasegawa⁵ studied the density of states and the total energy with the external field in the $(0, 0, 1)$, $(0, 1, 1)$, and $(1, 1, 1)$ directions for certain selected rational values of the resulting flux. Kunszt and Zee⁶ showed that for rational values of the flux the eigenvalue problem can be reduced to a one-dimensional hopping in momentum space. They then calculated the energy spectra and the density of states for various selected rational values of the flux states. These three works^{4–6} focused on a *discrete* set of (rational) magnetic field values. Here we are interested in obtaining results that are *continuous* functions of the applied field—valid for both commensurate and incommensurate flux values.

In this work, we focus on the isotropic 3D cubic lattice, namely, the hopping integrals in the x -, y -, and z -direction are the same and taken to be equal to one. The system is described by the Hamiltonian

$$H = \sum_{\langle ij \rangle} c_i^\dagger c_j \exp(iA_{ij}), \quad (1)$$

where $\langle ij \rangle$ refers to nearest-neighbor sites, and the phase $A_{ij} = 2\pi \int_i^j \mathbf{A} \cdot d\mathbf{l}$ is 2π times the line integral of the vector potential along the bond from i to j . Throughout this paper, the flux quantum $\Phi_0 = hc/e$ is set equal to one. The goal of this paper is to explore conceptually different viewpoints and approaches to study this interesting problem. Focusing on the hopping motion of electrons on the lattice, we first study the quantum interference between the phase factors of electron closed paths. This phenomenon is the source for the lowering of the total energy in a magnetic field.

In Sec. II, we examine the quantum interference effects originating from lattice path-integrals—defined as sums over magnetic phase factors on different electron closed paths. There, the physical meaning of these lattice path-integrals \mathcal{S}_{2l} and the techniques we use to compute them are discussed in detail. Results for \mathcal{S}_{2l} in an arbitrarily oriented field of any strength are also presented. Furthermore, we obtain the lattice path-integrals for several flux orientations by exactly summing an enormous number ($\sim 10^{29}$) of closed paths, each one weighted by its corresponding acquired phase factor.

In Sec. III, we present an analytical calculation of the total kinetic energy $E_T(\mathbf{B})$ of the half-filled Fermi sea of tight-binding electrons. We use two different approaches: one based on a direct series expansion for the energy² and the other on a moment expansion for the density of states.⁷ These two different methods yield the same results. Moreover, they provide different insights into the problem. For an arbitrary field orientation, analytic results for the total energy, in terms of the lattice path-integrals, are obtained. It is found that the lowest energy state is reached when the fluxes per plaquette on each one of the xy -, yz - and zx -planes are equal to $\Phi_0/2$. We also show the variations of the total energy E_T as a function of the flux, for various orientations of the magnetic field. Furthermore, we obtain an analytic expression for the total kinetic energy $E_T(\mathbf{B}, \nu)$ for any filling ν close to one half.

In Sec. IV, we investigate the magnetic moment $M(\mathbf{B})$ and orbital susceptibility $\chi(\mathbf{B})$ of this quantum system. For various flux orientations, we also obtain the zero-field susceptibility $\chi(\mu)$ as a function of the Fermi energy μ . We show that the magnetic response, in the presence of a strong periodic potential, is significantly different from the familiar Landau diamagnetism. The zero-field susceptibility $\chi(\mu)$ as a function of the Fermi energy μ exhibits a large diamagnetic (i.e., negative χ) response at very low electron filling. For increasing μ , $\chi(\mu)$ increases and fluctuates around zero. Paramagnetism prevails for large μ . Indeed, the orbital response is paramagnetic at and near half-filling ($\mu = 0$). We obtain the field dependence of $M(\mathbf{B})$ —which can be regarded as a generalized current in a multiply-connected geometry—and $\chi(\mathbf{B})$ at half-filling, and both show oscillations between para- and diamagnetic behaviors as a function of the flux. The frequencies of these oscillations, as functions of the flux, tend to decrease for increasing field.

In Sec. V, we summarize our results.

II. QUANTUM INTERFERENCE FROM SUMS OVER CLOSED PATHS: LATTICE PATH-INTEGRALS

A. Physical interpretation

The lattice path-integral of order $2l$ is defined as

$$\mathcal{S}_{2l} \equiv \sum_{\substack{\text{All closed } 2l\text{-step} \\ \text{lattice paths } \Gamma}} e^{i\Phi_\Gamma}, \quad (2)$$

where Φ_Γ is the sum over phases of the bonds on the path Γ of $2l$ steps starting and ending at the same site. Let $|\psi_i\rangle$ denote a localized one-site electron state centered at site i . It is not difficult to notice that \mathcal{S}_{2l} corresponds precisely to the quantum mechanical expectation value $\langle \psi_i | H^{2l} | \psi_i \rangle$, which summarizes the contribution to the electron kinetic energy of *all* closed paths of $2l$ -steps.

The physical meaning of \mathcal{S}_{2l} ($= \langle \psi_i | H^{2l} | \psi_i \rangle$) thus becomes clear. The Hamiltonian H is applied $2l$ times to the initial state $|\psi_i\rangle$, resulting in the new state $H^{2l}|\psi_i\rangle$ located at the end of the path traversing $2l$ lattice bonds. Because of the presence of a magnetic field, a magnetic phase factor $e^{iA_{ij}}$ is acquired by an electron when hopping through two adjacent sites i and j . \mathcal{S}_{2l} is nonzero only when the path ends at the starting site. In other words, \mathcal{S}_{2l} is the sum of the contributions from all closed paths of $2l$ steps starting and ending at the same site, each one weighted by its corresponding phase factor $e^{i\Phi_\Gamma}$ where $\Phi_\Gamma/2\pi$ is the *net* flux enclosed by the closed path Γ .

It is important to stress that Φ_Γ depends crucially on the traveling route of the path. For instance, Φ_Γ will be positive (negative) by traversing a polygon loop counterclockwise (clockwise). Therefore, quantum interference information contained in \mathcal{S}_{2l} arises because the phase factors of different closed paths, including those from all kinds of distinct loops and separate contributions from the same loop, interfere with each other. Sometimes, the phases corresponding to subloops of a main path cancel.

B. Analytical computational formalism

We will now compute the lattice path-integrals \mathcal{S}_{2l} . This is a difficult task since \mathcal{S}_{2l} involves an enormous number of different paths (growing rapidly when the order increases), each one given by its corresponding net magnetic phase

factor. We have considerably simplified this calculation by successively iterating the recursion relation and analyzing the symmetries of the problem.

We consider a unit spacing for the cubic lattice. The vector potential of a general magnetic field $\mathbf{B} = (B_x, B_y, B_z)$ can be written as

$$\mathbf{A} = \frac{1}{2}(zB_y - yB_z, xB_z - zB_x, yB_x - xB_y).$$

Let $a/2\pi$, $b/2\pi$, and $c/2\pi$ represent the three fluxes through the respective elementary plaquettes on the yz -, zx - and xy -planes. Thus, a flux configuration is specified by (a, b, c) .

From the definition of \mathcal{S}_{2l} , it is clear that: (i) \mathcal{S}_0 obviously equals 1, (ii) \mathcal{S}_{2l+1} are always zero because there is no path with an odd number of steps for returning an electron to its initial site, (iii) the \mathcal{S}_{2l} 's are gauge invariant, and (iv) in the absence of the magnetic field, \mathcal{S}_{2l} are just the total number of $2l$ -step paths on the cubic lattice starting and ending at the same site.

First, it is instructive to evaluate the first two lattice path-integrals. This will help clarify their physical meaning. For the two-step closed paths, and starting from any initial site, the electron retraces its first step on one of the six bonds connecting the initial site with its adjacent sites. This process can be designated symbolically by $(\cdot \leftrightarrow)$, where the dot (\cdot) indicates the initial site. The flux enclosed, of course, is zero. From these six closed paths of two steps each, we obtain

$$\mathcal{S}_2 = 6(\cdot \leftrightarrow) = 6e^{i0} = 6 = z,$$

where z stands for the coordination number of the cubic lattice.

For the four-step closed paths, we need to consider four different possibilities: (1) the electron retraces twice each one of the six bonds connecting the initial site with its nearest-neighboring sites $(\cdot \overleftrightarrow{\leftrightarrow})$; (2) after retracing once one of the six bonds connecting to the initial site, the electron retraces two steps on one of the other five bonds $(\leftrightarrow \cdot \leftrightarrow)$; (3) hopping first to one of the six adjacent sites, the electron retraces once one of the other five bonds (the one connecting to the initial site is excluded) and then returns to the original site $(\overleftarrow{\leftrightarrow} \leftrightarrow)$; and (4) the electron traverses either counterclockwise or clockwise on one of the four elementary square cells (connecting to the initial site) on the yz -, zx - and xy -planes respectively $[(\cdot \overleftarrow{\square} + \cdot \overrightarrow{\square})_{yz} + (\cdot \overleftarrow{\square} + \cdot \overrightarrow{\square})_{zx} + (\cdot \overleftarrow{\square} + \cdot \overrightarrow{\square})_{xy}]$. Thus

$$\begin{aligned} \mathcal{S}_4 &= 6(\cdot \overleftrightarrow{\leftrightarrow}) + 30(\leftrightarrow \cdot \leftrightarrow) + 30(\overleftarrow{\leftrightarrow} \leftrightarrow) \\ &\quad + 4[(\cdot \overleftarrow{\square} + \cdot \overrightarrow{\square})_{yz} + (\cdot \overleftarrow{\square} + \cdot \overrightarrow{\square})_{zx} + (\cdot \overleftarrow{\square} + \cdot \overrightarrow{\square})_{xy}] \\ &= (6 + 30 + 30)e^{i0} \\ &\quad + 4[(e^{ia} + e^{-ia}) + (e^{ib} + e^{-ib}) + (e^{ic} + e^{-ic})] \\ &= 66 + 8(\cos a + \cos b + \cos c). \end{aligned}$$

To compute \mathcal{S}_{2l} in a systematic manner, we first define the quantity $S_{p,q,r}^{(t)}$, which is the sum over all possible paths of t steps on which an electron may hop from the origin $(0, 0, 0)$ to site (p, q, r) . From the definition of $S_{p,q,r}^{(t)}$, it is straightforward to construct the following recurrence relation for $S_{p,q,r}^{(t+1)}$

$$S_{p,q,r}^{(t+1)} = \exp\left(\pm i \frac{qc - rb}{2}\right) S_{p\pm 1, q, r}^{(t)} + \exp\left(\pm i \frac{ra - pc}{2}\right) S_{p, q\pm 1, r}^{(t)} + \exp\left(\pm i \frac{pb - qa}{2}\right) S_{p, q, r\pm 1}^{(t)}. \quad (3)$$

This equation states that the site (p, q, r) can be reached by taking the $(t+1)$ th step from the six nearest-neighboring sites. The factors in front of the $S^{(t)}$'s account for the presence of the magnetic field. By recursively using Eq. (3), we obtain the recurrence relation for $S_{p,q,r}^{(t+2)}$ as

$$\begin{aligned} S_{p,q,r}^{(t+2)} &= 6S_{p,q,r}^{(t)} + \exp[\pm i(qc - rb)] S_{p\pm 2, q, r}^{(t)} + \exp[\pm i(ra - pc)] S_{p, q\pm 2, r}^{(t)} + \exp[\pm i(pb - qa)] S_{p, q, r\pm 2}^{(t)} \\ &\quad + 2\cos\left(\frac{c}{2}\right) \left[\exp\left(\pm i \frac{r(a-b) - (p-q)c}{2}\right) S_{p\pm 1, q\pm 1, r}^{(t)} + \exp\left(\mp i \frac{r(a+b) - (p+q)c}{2}\right) S_{p\pm 1, q\mp 1, r}^{(t)} \right] \\ &\quad + 2\cos\left(\frac{b}{2}\right) \left[\exp\left(\pm i \frac{q(c-a) - (r-p)b}{2}\right) S_{p\pm 1, q, r\pm 1}^{(t)} + \exp\left(\mp i \frac{q(c+a) - (r+p)b}{2}\right) S_{p\pm 1, q, r\mp 1}^{(t)} \right] \\ &\quad + 2\cos\left(\frac{a}{2}\right) \left[\exp\left(\pm i \frac{p(b-c) - (q-r)a}{2}\right) S_{p, q\pm 1, r\pm 1}^{(t)} + \exp\left(\mp i \frac{p(b+c) - (q+r)a}{2}\right) S_{p, q\pm 1, r\mp 1}^{(t)} \right]. \quad (4) \end{aligned}$$

We will now use Eq. (4) as the basic recurrence relation in our iteration scheme. Without loss of generality and for convenience, we choose the origin $(0, 0, 0)$ to be our starting site. The initial conditions then read $S_{0,0,0}^{(0)} = 1$ and $S_{p,q,r}^{(0)} = 0$ for other (p, q, r) 's. It is evident that S_{2l} is just equal to $S_{0,0,0}^{(2l)}$. Putting $t = 0$ in Eq. (4), we directly have $S_{0,0,0}^{(2)} = 6$,

$$\begin{aligned} S_{1,1,0}^{(2)} &= S_{1,-1,0}^{(2)} = S_{-1,1,0}^{(2)} = S_{-1,-1,0}^{(2)} = 2 \cos\left(\frac{c}{2}\right), \\ S_{1,0,1}^{(2)} &= S_{1,0,-1}^{(2)} = S_{-1,0,1}^{(2)} = S_{-1,0,-1}^{(2)} = 2 \cos\left(\frac{b}{2}\right), \\ S_{0,1,1}^{(2)} &= S_{0,1,-1}^{(2)} = S_{0,-1,1}^{(2)} = S_{0,-1,-1}^{(2)} = 2 \cos\left(\frac{a}{2}\right), \end{aligned}$$

and

$$S_{2,0,0}^{(2)} = S_{-2,0,0}^{(2)} = S_{0,2,0}^{(2)} = S_{0,-2,0}^{(2)} = S_{0,0,2}^{(2)} = S_{0,0,-2}^{(2)} = 1.$$

Using the above results for the $S_{p,q,r}^{(2)}$'s and putting $t = 2$ in Eq. (4), we then obtain the $S_{p,q,r}^{(4)}$'s. In general, by following this procedure we can obtain $S_{0,0,0}^{(2l)}$ to any desired l . The properties discussed below will make the computation of $S_{0,0,0}^{(2l)}$ quite efficient.

For a given l , a nonzero $S_{p,q,r}^{(2l)}$ exists only on those p, q , and r satisfying $|p| + |q| + |r| = 0, 2, \dots, 2l$. This stems from the fact that only the sites (p, q, r) satisfying this condition can be reached by an electron after $2l$ hops from $(0, 0, 0)$. The total number of these sites is

$$N_T^{(2l)} = \frac{16l^3 + 24l^2 + 14l + 3}{3}.$$

Among the $S_{p,q,r}^{(2l)}$'s, we find the following symmetries hold for any l . We omit the superscript $(2l)$ below.

$$\begin{aligned} S_{p,q,r}(a, b, c) &= S_{-p,-q,-r}(a, b, c), \\ S_{-p,q,r}(a, b, c) &= S_{p,-q,-r}(a, b, c), \\ S_{p,-q,r}(a, b, c) &= S_{-p,q,-r}(a, b, c), \\ S_{p,q,-r}(a, b, c) &= S_{-p,-q,r}(a, b, c), \end{aligned}$$

$$S_{p,q,r}(a, b, c) = S_{-p,q,r}(-a, b, c) = S_{p,-q,r}(a, -b, c) = S_{p,q,-r}(a, b, -c),$$

and

$$S_{p,q,r}(a, b, c) = S_{p,r,q}(a, c, b) = S_{r,p,q}(b, c, a) = S_{q,p,r}(b, a, c) = S_{q,r,p}(c, a, b) = S_{r,q,p}(c, b, a).$$

We can therefore reduce our calculation to the $S^{(2l)}$'s at sites (p, q, r) in the first octant with $p \geq q \geq r \geq 0$. Thus, the total number of the independent $S_{p,q,r}^{(2l)}$ is

$$N_I^{(2l)} = \frac{l^3 + 6l^2 + 12l + 9 - n}{9}$$

for $l = 3m + n$, where m are non-negative integers and $n = 0, 1, 2$. Thus the number of the $S^{(2l)}$'s to be computed is significantly reduced (about a factor of 48) compared to that of the whole $S_{p,q,r}^{(2l)}$.

Finally, it is worthwhile to note that to obtain the lattice path-integrals up to S_{2L} , it is sufficient to compute the $S_{p,q,r}^{(L)}$'s for $0 \leq p + q + r \leq L$ when L is even and the $S_{p,q,r}^{(L+1)}$'s for $0 \leq p + q + r \leq L - 1$ when L is odd. To be more specific, in doing the iteration of $S_{p,q,r}^{(2l)}$ for $L/2 \leq l \leq L$, we need only to concern ourselves with those $S_{p,q,r}^{(2l)}$'s with $p + q + r = 0, 2, \dots, 2(L - l)$.

C. Results for lattice path-integrals with general flux orientations

For the general flux orientation (a, b, c) , we have obtained \mathcal{S}_{2l} up to $2l = 20$. Here: $\sum_{(\alpha)}$ denote sums over $\alpha = a, b, c$; $\sum_{(\alpha\beta)}$ denote sums over $(\alpha\beta) = (ab), (bc), (ca)$; and $\sum_{(\alpha\beta\gamma)}$ denote sums over $(\alpha\beta\gamma) = (abc), (bca), (cab)$. Also, for instance, the term $\cos(\alpha \pm \beta)$ means $\cos(\alpha + \beta) + \cos(\alpha - \beta)$. Below we present the results for $\mathcal{S}_4, \mathcal{S}_6, \mathcal{S}_8$, and \mathcal{S}_{10} .

$$\begin{aligned}
\mathcal{S}_4 &= 66 + 8 \sum_{(\alpha)} \cos \alpha, \\
\mathcal{S}_6 &= 876 + \sum_{(\alpha)} [240 \cos \alpha + 24 \cos 2\alpha] + 24 \sum_{(\alpha\beta)} \cos(\alpha \pm \beta) + 12 \cos(a + b + c) + 12 \sum_{(\alpha\beta\gamma)} \cos(\alpha + \beta - \gamma), \\
\mathcal{S}_8 &= 12978 + \sum_{(\alpha)} [5632 \cos \alpha + 1000 \cos 2\alpha + 96 \cos 3\alpha + 16 \cos 4\alpha] \\
&\quad + \sum_{(\alpha\beta)} [1120 \cos(\alpha \pm \beta) + 112 \cos(2\alpha \pm \beta) + 112 \cos(\alpha \pm 2\beta) + 32 \cos(2\alpha \pm 2\beta)] + 576 \cos(a + b + c) \\
&\quad + \sum_{(\alpha\beta\gamma)} [576 \cos(\alpha + \beta - \gamma) + 64 \cos(2\alpha + \beta \pm \gamma) + 64 \cos(2\alpha - \beta \pm \gamma) \\
&\quad + 16 \cos(\alpha + 2\beta \pm 2\gamma) + 16 \cos(\alpha - 2\beta \pm 2\gamma)], \\
\mathcal{S}_{10} &= 208836 + \sum_{(\alpha)} [124080 \cos \alpha + 30040 \cos 2\alpha + 5040 \cos 3\alpha + 1160 \cos 4\alpha + 160 \cos 5\alpha + 40 \cos 6\alpha] \\
&\quad + \sum_{(\alpha\beta)} [36680 \cos(\alpha \pm \beta) + 6800 \cos(2\alpha \pm \beta) + 6800 \cos(\alpha \pm 2\beta) + 2160 \cos(2\alpha \pm 2\beta) \\
&\quad + 600 \cos(3\alpha \pm \beta) + 600 \cos(\alpha \pm 3\beta) + 240 \cos(3\alpha \pm 2\beta) + 240 \cos(2\alpha \pm 3\beta) + 80 \cos(4\alpha \pm \beta) \\
&\quad + 80 \cos(\alpha \pm 4\beta) + 60 \cos(2\alpha \pm 4\beta) + 60 \cos(2\alpha \pm 4\beta) + 40 \cos(3\alpha \pm 3\beta)] + 19860 \cos(a + b + c) \\
&\quad + \sum_{(\alpha\beta\gamma)} [19860 \cos(\alpha + \beta - \gamma) + 4040 \cos(2\alpha + \beta \pm \gamma) + 4040 \cos(2\alpha - \beta \pm \gamma) \\
&\quad + 1280 \cos(\alpha + 2\beta \pm 2\gamma) + 1280 \cos(\alpha - 2\beta \pm 2\gamma) + 400 \cos(3\alpha + \beta \pm \gamma) + 400 \cos(3\alpha - \beta \pm \gamma) \\
&\quad + 160 \cos(\alpha + 2\beta \pm 3\gamma) + 160 \cos(\alpha - 2\beta \pm 3\gamma) + 160 \cos(\alpha + 3\beta \pm 2\gamma) + 160 \cos(\alpha - 3\beta \pm 2\gamma) \\
&\quad + 40 \cos(4\alpha + \beta \pm \gamma) + 40 \cos(4\alpha - \beta \pm \gamma) + 40 \cos(3\alpha + 2\beta \pm 2\gamma) + 40 \cos(3\alpha - 2\beta \pm 2\gamma) \\
&\quad + 40 \cos(\alpha + 4\beta \pm 2\gamma) + 40 \cos(\alpha - 4\beta \pm 2\gamma) + 40 \cos(\alpha + 2\beta \pm 4\gamma) + 40 \cos(\alpha - 2\beta \pm 4\gamma) \\
&\quad + 20 \cos(4\alpha + 2\beta \pm 2\gamma) + 20 \cos(4\alpha - 2\beta \pm 2\gamma) + 20 \cos(\alpha + 3\beta \pm 3\gamma) + 20 \cos(\alpha - 3\beta \pm 3\gamma)].
\end{aligned}$$

We have also worked out a considerable number of lattice path-integrals (up to the 40th order) for various special orientations of the flux. The results for $\mathcal{S}_4, \mathcal{S}_6, \dots, \mathcal{S}_{12}$ are listed in Table I. The results for $\mathcal{S}_{14}, \mathcal{S}_{16}, \dots, \mathcal{S}_{40}$ are not presented.

III. TOTAL KINETIC ENERGY

We now proceed to calculate the total kinetic energy E_T of the half-filled Fermi sea. We do this by using a series expansion of the total energy. We also present an alternative approach based on a moment expansion of the density of states. Through these two different approaches, we show that our goal here—the calculation of $E_T(\mathbf{B})$ —is reduced to the evaluation of the lattice path-integrals \mathcal{S}_{2l} .

A. Series expansion for the total energy

Let us work on the $\{|\psi_i\rangle\}$ basis. At half-filling, the total kinetic energy of noninteracting spinless electrons is the sum of the lowest $N/2$ eigenvalues, where N is the total number of sites. Since the energy spectrum of the cubic lattice is symmetric under $\{E\} \rightarrow \{-E\}$, we can write the total energy per site as

$$E_T = \frac{1}{N} \sum_{E < 0} E = -\frac{z}{2N} \text{Tr} \left| \frac{H_0}{z} \right|. \quad (5)$$

Here Tr denotes the trace and H_0 is the corresponding diagonalized Hamiltonian of H . Notice that the absolute value is typically defined for scalar numbers. In this case, $|H_0/z|$ refers to an operator obtained by taking the absolute value of every matrix element of the operator H_0/z . Noting that $-I \leq |H_0/z| \leq I$, we expand $|H_0/z|$ into a series in terms of Chebyshev polynomials $T_{2k}(H_0/z)$ as

$$\left| \frac{H_0}{z} \right| = \frac{2}{\pi} I + \frac{4}{\pi} \sum_{n=1}^{\infty} \frac{(-1)^{n+1}}{4n^2 - 1} T_{2n} \left(\frac{H_0}{z} \right), \quad (6)$$

where I represents the identity operator. Exploiting the equality

$$T_{2n} \left(\frac{H_0}{z} \right) = (-1)^n n \sum_{l=0}^n \Omega_l H_0^{2l}, \quad (7)$$

where

$$\Omega_l = \left(\frac{-4}{z^2} \right)^l \frac{(n+l-1)!}{(2l)!(n-l)!},$$

we obtain from Eqs. (5-7)

$$E_T = -\frac{z}{\pi} \left[1 - \frac{2}{N} \sum_{n=1}^{\infty} \frac{n}{4n^2 - 1} \left(\sum_{l=0}^n \Omega_l (\text{Tr} H^{2l}) \right) \right], \quad (8)$$

where we have replaced $\text{Tr}(H_0^{2l})$ by $\text{Tr}(H^{2l})$, as they are equal to each other.

Assuming periodic boundary conditions on the lattices, we have

$$\text{Tr} H^{2l} = N \langle \psi_i | H^{2l} | \psi_i \rangle. \quad (9)$$

The total kinetic energy per site is then given by

$$E_T(a, b, c) = -\frac{z}{\pi} \left[1 - 2 \sum_{n=1}^L \frac{n}{4n^2 - 1} \left(\sum_{l=0}^n \Omega_l \mathcal{S}_{2l}(a, b, c) \right) \right], \quad (10)$$

where we have assumed the highest order of the lattice path-integral obtained is $2L$. The above result is exact when $L = \infty$. Truncations at high values of L provide excellent approximations to the $L = \infty$ case, because the terms corresponding to L larger than either 4, 5, or 6 (depending on the orientation of the field) are negligible. Our results for the general field orientation (a, b, c) of E_T include all terms up to $L = 10$. For the special flux configurations $(0, 0, \phi)$, $(0, \phi, \phi)$, (ϕ, ϕ, ϕ) , $(\phi, \phi, -2\phi)$, and (π, π, ϕ) , we obtain all terms up to $L = 20$. Terms up to $L = 10$ (corresponding to \mathcal{S}_{20}) include contributions originating from $\sim 10^{14}$ three-dimensional closed paths, while terms up to $L = 20$ (corresponding to \mathcal{S}_{40}) include contributions coming from $\sim 10^{29}$ closed paths in a 3D cubic lattice. Each one of these closed paths is weighted by its corresponding magnetic phase factor.

Note that, by construction, the lattice path-integrals are local quantities and are valid for any value of ϕ . The periodic boundary conditions make the lattice path-integrals homogeneous (i.e., translationally invariant) and are unrelated to the imposition of a Bloch theorem. In contrast to most works studying tight-binding electrons in a magnetic field, here we never invoke a k -space or reciprocal space: our sums are all defined in direct space.

B. Moment expansion for the density of states

Here we analytically apply the method of moment expansion to obtain the total energy E_T . The starting point now is the one-particle Green's function $G_{ii}(E) \equiv \langle \psi_i | (E - H)^{-1} | \psi_i \rangle$, which can be expressed as

$$G_{ii}(E) = \frac{1}{E} \sum_{l=0}^{\infty} \frac{\langle \psi_i | H^{2l} | \psi_i \rangle}{E^{2l}} = \frac{1}{E} \sum_{l=0}^{\infty} \frac{\mathcal{S}_{2l}}{E^{2l}}. \quad (11)$$

The nonzero $2l$ -th moment \mathcal{M}_{2l} of the density of states $\rho(E)$ is given by

$$\mathcal{M}_{2l} = \int_{-z}^z \left(\frac{E}{z}\right)^{2l} \rho(E) dE. \quad (12)$$

Taking into account the relation between $\rho(E)$ and the imaginary part of the Green's function, it can be derived that

$$\mathcal{M}_{2l} = \frac{\mathcal{S}_{2l}}{z^{2l}}. \quad (13)$$

After the change of variables $\omega = E/z$, Eq. (12) can be rewritten as

$$\mathcal{M}_{2l} = \int_{-1}^1 \omega^{2l} \tilde{\rho}(\omega) d\omega, \quad (14)$$

where $\tilde{\rho}(\omega) = z \rho(\omega z)$.

We now expand $\tilde{\rho}(\omega)$ in a series of Chebyshev polynomials weighted by $1/\sqrt{1-\omega^2}$ as

$$\tilde{\rho}(\omega) = \sum_{k=0}^{\infty} C_{2k} \frac{T_{2k}(\omega)}{\sqrt{1-\omega^2}}. \quad (15)$$

Substituting Eq. (15) into Eq. (14) and using for $l \geq k$

$$\int_{-1}^1 \frac{\omega^{2l} T_{2k}(\omega)}{\sqrt{1-\omega^2}} d\omega \equiv I_{2l,2k} = \frac{(2l)! \pi}{4^l (l-k)! (l+k)!}, \quad (16)$$

we obtain

$$\mathcal{M}_{2l} = \sum_{k=0}^l C_{2k} I_{2l,2k}. \quad (17)$$

Given the moments up to \mathcal{M}_{2L} , the coefficients C_{2k} , for $k = 0, \dots, L$, can then be exactly determined one by one in terms of the moments. For instance,

$$C_0 = \frac{\mathcal{M}_0}{I_{0,0}} = \frac{1}{\pi},$$

$$C_2 = \frac{\mathcal{M}_2 - C_0 I_{2,0}}{I_{2,2}} = -\frac{4}{3\pi},$$

and

$$\begin{aligned} C_4 &= \frac{\mathcal{M}_4 - C_0 I_{4,0} - C_2 I_{4,2}}{I_{4,4}} \\ &= \frac{4}{27\pi} \left[1 + \frac{2}{3} (\cos a + \cos b + \cos c) \right]. \end{aligned}$$

In general, every C_{2k} can be computed from the previous ones by

$$C_{2k} = \frac{1}{I_{2k,2k}} \left(\mathcal{M}_{2k} - \sum_{i=0}^{k-1} C_{2i} I_{2k,2i} \right). \quad (18)$$

Noting that at half-filling the total energy E_T is

$$E_T = \int_{-z}^0 E \rho(E) dE, \quad (19)$$

and using the result

$$\int_{-1}^0 \frac{\omega T_{2k}(\omega)}{\sqrt{1-\omega^2}} d\omega = \frac{(-1)^k}{(2k-1)(2k+1)},$$

we therefore obtain the following expression for the total kinetic energy

$$E_T(a, b, c) = z \sum_{k=0}^L \frac{(-1)^k}{(2k-1)(2k+1)} C_{2k}(a, b, c). \quad (20)$$

It is interesting to notice that Eqs. (10) and (20) lead to the same result for the total energy E_T , even though we used quite different approaches. Both results are exact when $L = \infty$. However, terms with k larger than 4, 5, or 6 (depending on the field orientation) provide negligible contributions to the sum. Our results for the general field orientation (a, b, c) of $E_T(a, b, c)$ include all terms up to $L = 10$, while for the five special flux configurations studied below (Sec. III.C), we include all terms up to $L = 20$.

C. The lowest-energy flux state and E_T for various flux orientations

Substituting the expressions for the $\mathcal{S}_{2l}(a, b, c)$'s into Eq. (10) or the results for the $C_{2l}(a, b, c)$'s into Eq. (20), we find that the lowest energy state is reached when $a = b = c = \pi$ (namely, a half flux quantum per plaquette on the yz -, zx - and xy -planes). We thus provide an *explicit analytic derivation for the absolute minimum energy of the flux state*. The result is consistent with a theorem proved by Lieb.³

We also obtain the total energy $E_T(\phi)$ as a *continuous* function of the flux ϕ for the following flux orientations: $(0, 0, \phi)$, $(0, \phi, \phi)$, (ϕ, ϕ, ϕ) , $(\phi, \phi, -2\phi)$, and the asymmetric case (π, π, ϕ) . Notice that the field direction of (ϕ, ϕ, ϕ) is perpendicular to that of $(\phi, \phi, -2\phi)$. These results are plotted in Fig. 1. They are calculated through Eq. (20) by using their respective C_{2k} 's for $2k = 0, 2, 4, \dots, 40$. Thus, we have added the contributions of $\sim 10^{29}$ electron closed paths in a 3D cubic lattice, each one weighted by its magnetic phase factor.

For comparison purposes, we also present $E_T^{(2D)}(\phi)$ for the 2D case, obtained by using the corresponding $C_{2k}^{(2D)}$'s up to $C_{76}^{(2D)}$. This corresponds to summing over $\sim 10^{44}$ electron closed paths in a 2D square lattice, each one with its corresponding phase factor. Note that the absolute minimum of $E_T(\phi)$ occurs at $\phi = \pi$ in all of these flux orientations, except for the orientation $(0, 0, \phi)$ in 3D. It becomes clear that hopping in an extra dimension drastically changes the properties found in strictly two-dimensional systems.

In Fig. 2, we plot the total kinetic energy of electrons at half-filling E_T for the 3D cubic lattice for various field orientations versus the order of the highest-order lattice path-integral used to calculate them. For comparison, we also show the numerical values of E_T obtained in Ref. 5, which mostly has only three significant figures. The E_T reach steady values which are consistent, within $\sim 2\%$, with numerical ones for lattice path-integrals of order $2L$ equal to either 4, 6, or 8, depending on the orientation of the field. Higher order lattice path-integrals provide negligible contributions to E_T . For instance, for $(0, 0, 0)$ both approaches give the same result, within $\sim 0.5\%$, for $2L \geq 4$.

D. Total energy for any filling

The approach described in section III.B can be directly generalized to calculate the total energy $E_T(\nu)$ for *any* electron filling ν ($0 \leq \nu \leq 1/2$) as

$$E_T(\nu) = \int_{-z}^{\mu} E \rho(E) dE = z \int_{-1}^{\mu/z} \omega \tilde{\rho}(\omega) d\omega, \quad (21)$$

where the Fermi energy μ is determined by

$$\nu = \int_{-z}^{\mu} \rho(E) dE = \int_{-1}^{\mu/z} \tilde{\rho}(\omega) d\omega. \quad (22)$$

Utilizing Eq. (15) and carrying out the integrals, we obtain

$$E_T(\nu) = -\frac{z}{\pi} \sin \theta - \frac{z}{2} \sum_{k=1}^L C_{2k} \left[\frac{\sin[(2k-1)\theta]}{2k-1} + \frac{\sin[(2k+1)\theta]}{2k+1} \right], \quad (23)$$

where $\theta = \arccos(\mu/z)$ ($\pi \geq \theta \geq \pi/2$), and given ν , θ can be solved from the following equation

$$\nu = 1 - \frac{\theta}{\pi} - \sum_{k=1}^L C_{2k} \frac{\sin(2k\theta)}{2k}. \quad (24)$$

Note that $0 \leq \nu \leq 1/2$ corresponds to $-z \leq \mu \leq 0$ and $\pi \geq \theta \geq \pi/2$. Writing $\nu = 1/2 - \delta$ and $\theta = \pi/2 + \eta$, Eqs. (23) and (24) can then be rewritten as

$$E_T \left(\frac{1}{2} - \delta \right) = -\frac{z}{\pi} \cos \eta + \frac{z}{2} \sum_{k=1}^L (-1)^k C_{2k} \left[\frac{\cos[(2k-1)\eta]}{2k-1} - \frac{\cos[(2k+1)\eta]}{2k+1} \right] \quad (25)$$

and

$$\delta = \frac{\eta}{\pi} + \sum_{k=1}^L (-1)^k C_{2k} \frac{\sin(2k\eta)}{2k}. \quad (26)$$

In the small δ limit (i.e., the electron filling ν is close to one half and η is very small) $\sin(2k\eta) \simeq 2k\eta$; we then have

$$\eta \simeq \frac{\pi}{1 + \pi \mathcal{C}(a, b, c)} \delta, \quad (27)$$

where

$$\mathcal{C}(a, b, c) = \sum_{k=1}^L (-1)^k C_{2k}(a, b, c).$$

Therefore, using the approximation $\cos[(2k \pm 1)\eta] \simeq 1 - (2k \pm 1)^2 \eta^2 / 2$, we obtain the total energy $E_T(1/2 - \delta)$ close to (and below) half-filling

$$\begin{aligned} E_T \left(\frac{1}{2} - \delta \right) &\simeq -\frac{z}{\pi} \cos \left(\frac{\pi}{1 + \pi \mathcal{C}} \delta \right) + z \sum_{k=1}^L \frac{(-1)^k}{(2k-1)(2k+1)} C_{2k} + \frac{z}{2} \frac{\pi^2 \mathcal{C}}{(1 + \pi \mathcal{C})^2} \delta^2 \\ &\simeq E_T \left(\frac{1}{2} \right) + \frac{z}{\pi} \left[1 - \cos \left(\frac{\pi}{1 + \pi \mathcal{C}} \delta \right) \right] + \frac{z}{2} \frac{\pi^2 \mathcal{C}}{(1 + \pi \mathcal{C})^2} \delta^2. \end{aligned} \quad (28)$$

Finally, by differentiating both E_T in Eq. (23) and ν in Eq. (24) with respect to μ , we can establish the following identity

$$\frac{dE_T}{d\mu} = \mu \frac{d\nu}{d\mu}. \quad (29)$$

It is worthwhile to emphasize that the formalism described in this section is equally applicable to the 2D square lattice case.

IV. MAGNETIC MOMENT AND ORBITAL SUSCEPTIBILITY

In this section we investigate two experimentally accessible observables, namely, the magnetic moment M and the orbital susceptibility χ of this quantum system. It is well known⁸ that at absolute zero temperature M and χ are given by the first- and second-order derivatives of the total energy

$$M = -\frac{\partial E_T}{\partial B} \quad (30)$$

and

$$\chi = -\frac{\partial^2 E_T}{\partial B^2}. \quad (31)$$

With our analytical results for E_T at hand, equations (30) and (31) provide a straightforward way to study these important quantities for any orientation of the externally applied field. For illustration purposes, below we will focus on the following flux orientations: $(0, 0, \phi)$, $(0, \phi, \phi)$, (ϕ, ϕ, ϕ) , and $(\phi, \phi, -2\phi)$. It will be seen that the magnetic response, in the presence of a strong periodic potential, is significantly different from the familiar Landau diamagnetism of a 2D electron gas, where $-\chi$ has its largest value at $B = 0$ and its vicinity and decreases *monotonically* as B is increased.

A. Zero-field susceptibility $\chi(\mu) = \chi(\phi = 0, \mu)$ versus Fermi energy μ

When we increase the electron filling factor ν , the Fermi energy μ increases. We therefore first study the zero-field susceptibility $\chi(\mu) = \chi(\phi = 0, \mu)$ as a function of μ through

$$\chi(\mu) = -\left. \frac{\partial^2 E_T}{\partial B^2} \right|_{B=0}. \quad (32)$$

From Eq. (23), we readily obtain

$$\chi(\mu) = \frac{z}{2} \sum_{k=2}^L \left(\left. \frac{d^2 C_{2k}(\phi)}{d\phi^2} \right|_{\phi=0} \right) \left[\frac{\sin[(2k-1)\theta]}{2k-1} + \frac{\sin[(2k+1)\theta]}{2k+1} \right], \quad (33)$$

where $d^2 C_{2k}(\phi)/d\phi^2|_{\phi=0}$ can be easily computed for each of the flux orientations under consideration.

In Fig. 3 we plot the negative of the susceptibility $-\chi$ as a function of the Fermi energy μ for various flux configurations. Large diamagnetic (i.e., negative) susceptibilities are observed at very low electron filling. For increasing μ , the quantity $-\chi$ decreases and fluctuates around zero. For μ larger than a certain value ($\simeq -3.2$), paramagnetism prevails. Indeed, the orbital response is weakly paramagnetic at half-filling ($\mu = 0$). These results are in qualitative agreement with the observations of Skudlarski and Vignale⁴ based on calculating the current-current correlation function. Furthermore, note that the absolute value of χ for $(0, \phi, \phi)$ is always twice that for $(0, 0, \phi)$; $|\chi|$ for (ϕ, ϕ, ϕ) is always three times that for $(0, 0, \phi)$; and $|\chi|$ for $(\phi, \phi, -2\phi)$ is twice that for (ϕ, ϕ, ϕ) . These results clearly reflect the orbital origin of the susceptibility.

B. Field-dependent $M(\phi)$ and $\chi(\phi)$ at $\nu = \frac{1}{2}$

We now focus on the system at half-filling and examine the *continuous* dependence of the magnetic moment M and susceptibility χ on the magnetic flux ϕ . Employing Eq. (20) for $E_T(\phi)$, we can directly obtain

$$-M(\phi) = \frac{dE_T(\phi)}{d\phi} = z \sum_{k=0}^L \frac{(-1)^k}{(2k-1)(2k+1)} \frac{dC_{2k}(\phi)}{d\phi}, \quad (34)$$

and

$$-\chi(\phi) = \frac{d^2 E_T(\phi)}{d\phi^2} = z \sum_{k=0}^L \frac{(-1)^k}{(2k-1)(2k+1)} \frac{d^2 C_{2k}(\phi)}{d\phi^2}. \quad (35)$$

The results for four different flux orientations are shown in Fig. 4. Let us look at $-M(\phi) = -M(\phi, \nu = 1/2)$ first. Starting from $\phi = 0$, $-M(\phi)$ decreases from zero and remains negative with some fluctuations. There are then some irregular ‘‘sine-function-shaped’’ oscillations present. These low-field oscillations in $-M(\phi)$ are observed for all orientations shown in Fig. 4. For the $(0, 0, \phi)$ flux orientation, $-M$ has a positive value for $\phi/2\pi \approx 0.3-0.5$, reaching zero at $\phi = \pi$. On the other hand, for $(0, \phi, \phi)$, (ϕ, ϕ, ϕ) and $(\phi, \phi, -2\phi)$, $-M$ is mostly negative for low fields ($\phi/2\pi \approx 0-0.1$), oscillates around zero for intermediate fields ($\phi/2\pi \approx 0.1-0.3$), is negative for larger fields ($\phi/2\pi \approx 0.3-0.5$), and reaches zero at $\phi = \pi$. At relatively large flux values ($\phi/2\pi \approx 0.4-0.5$), $-M$: decreases to zero (at $\phi = \pi$) from a positive value for $(0, 0, \phi)$; and increases to zero (at $\phi = \pi$) from a negative value for $(0, \phi, \phi)$, (ϕ, ϕ, ϕ) , and $(\phi, \phi, -2\phi)$.

The field-dependent orbital magnetic susceptibility, $-\chi = -\chi(\phi, \nu = 1/2)$, fluctuates somewhat evenly around zero in the low-field regime. However, $-\chi$ fluctuates less, and around a small negative value for the flux orientation $(0, 0, \phi)$, where only one plane (xy -plane) is penetrated by the flux. The fluctuations are more pronounced in the flux orientations: $(0, \phi, \phi)$, (ϕ, ϕ, ϕ) , and $(\phi, \phi, -2\phi)$, where at least two perpendicular planes are affected by the field. As the flux is raised, $-\chi$ tends to fluctuate less and: (i) a crossover from diamagnetism to paramagnetism is observed in the configuration $(0, 0, \phi)$; and, on the other hand, (ii) a crossover from paramagnetism to diamagnetism is observed in the orientations $(0, \phi, \phi)$, (ϕ, ϕ, ϕ) , and $(\phi, \phi, -2\phi)$. In other words, at $\phi = \pi$, the magnetic response is weakly paramagnetic in the flux configuration $(0, 0, \phi)$, while the other three orientations provide a strong diamagnetic response in the lattice.

Figure 4 suggests that, for both M and χ , the following four quantities tend to grow larger with the increase of planes exposed to the field: the number of oscillations, the frequency of the oscillations as a function of the flux, the

number of nodes, and the amplitude of the oscillations. For instance, $M(\phi, \phi, \phi)$ oscillates more rapidly and strongly than $M(0, \phi, \phi)$, which at the same time oscillates more rapidly and strongly than $M(0, 0, \phi)$. A similar general trend is observed between $\chi(\phi, \phi, \phi)$, $\chi(0, \phi, \phi)$, and $\chi(0, 0, \phi)$. These features can be understood intuitively: the more perpendicular planes are exposed to the flux, the more strongly M and χ will be affected.

V. SUMMARY

In conclusion, we present an investigation of quantum interference phenomena of tight-binding electrons on the 3D cubic lattice in a *continuously-tunable* magnetic field with *arbitrary orientation*. Previous work on this problem focused on a *discrete* set of (rational) magnetic field values. We study the total kinetic energy, and subsequently the magnetic moment and orbital susceptibility. The main results include: (1) an analytic study of electron quantum interference effects resulting from sums over magnetic phase factors associated with 3D closed paths, (2) a very efficient computation of these “lattice path-integrals” \mathcal{S}_{2l} in closed-form expressions, (3) explicit analytic expressions, in terms of the lattice path-integrals, for the Fermi-sea ground-state energy E_T as a function of the fluxes for electron fillings ν at and near one half, (4) the 3D lattice path-integrals to very high order and the total energies in various flux orientations, (5) the investigation of the zero-field orbital susceptibility $\chi(\mu)$ as a function of the Fermi energy μ , and (6) the magnetic moment $M(\phi)$ and susceptibility $\chi(\phi)$ as functions of the flux, both at half-filling.

We find that the absolute minimum of $E_T(\phi)$ at half-filling occurs at $\phi = \pi$ in all of the flux orientations under consideration, except for the configuration $(0, 0, \phi)$ in 3D. It becomes evident that hopping in an additional direction drastically changes the properties found in strictly two-dimensional systems. It is also seen that the magnetic response, in the presence of a strong periodic potential, is significantly distinct from the familiar Landau diamagnetism—where in a 2D electron gas $-\chi$ takes the largest value close to $B = 0$, and decreases monotonically with increasing B . For the zero-field susceptibility $\chi(\mu)$, diamagnetism dominates in spite of small fluctuations of $\chi(\mu)$ around zero for small electron filling ν . On the average, with increasing μ , the quantity $-\chi(\mu)$ *non-monotonically* decreases from a large positive (diamagnetic) value to a relatively small negative (paramagnetic) value. For $\mu \geq -3.2$, the orbital response becomes paramagnetic. Both the field-dependent $-M(\phi)$ and $-\chi(\phi)$ exhibit irregular oscillations according to the direction of the field. For the four flux orientations $(0, 0, \phi)$, $(0, \phi, \phi)$, (ϕ, ϕ, ϕ) , and $(\phi, \phi, -2\phi)$, the magnetic moment $M(\phi)$ is always zero at $\phi = 0$ and π ; and paramagnetism ($\chi > 0$) exists at $\phi = 0$ for all these flux orientations. However, when $\phi/2\pi = 1/2$, the magnetic response is paramagnetic for the flux configuration $(0, 0, \phi)$, and diamagnetic for the other three orientations.

Here, we add a remark on the quantity $dE_T(\phi)/d\phi$. It is known that at zero temperature the persistent current⁹ in a metal ring threaded by a magnetic flux φ is proportional to the sum over the contributions of $\partial E_n/\partial\varphi$ from all occupied states, where E_n is the eigenstate energy. We therefore can regard $dE_T(\phi)/d\phi$ as a generalized “current” in this multiply-connected lattice system.

An approach commonly employed in recent years to study electrons in a magnetic field $\phi = p/q$ (e.g., Refs. 4-6) uses the Bloch theorem and maps the problem into a $q \times q$ matrix problem—related to a $q \times q$ cell with periodic boundary conditions (PBC) in the actual lattice. Thus, for $\phi = 1/2$, the electron energy levels are determined by considering a 2×2 cell with PBC in the lattice and diagonalizing a 2×2 matrix. This approach presents a problem for any irrational field, since $q \rightarrow \infty$, and a periodic cell cannot be realized. We do not follow this approach, thus, we can explicitly consider a *continuum* of values of ϕ , without treating irrational numbers on a special footing.

Our lattice path-integrals are local quantities. By construction, they are valid for *any* value of the magnetic field. The PBC we impose [in Eq. (9)] are only designed to make these lattice path-integrals homogeneous (i.e., translationally invariant) and have nothing to do with the imposition of a Bloch theorem. Indeed, in contrast to most works studying electrons in a magnetic field, here we never invoke any k-space or momentum-space: our sums over closed paths (lattice path-integrals) are all explicitly defined in real space.

The lattice path-integrals obtained here are “many-loop” generalizations of the standard “one-loop” Aharonov-Bohm-type argument, where the electron wave function picks up a phase factor $e^{i\Phi}$ each time it travels around a closed loop enclosing a net flux Φ . The evaluation of these lattice path-integrals enables us to analytically obtain the total energies, magnetic moments, and orbital susceptibilities of the corresponding flux states. The spirit of our approach follows Feynman’s programme: to derive physical quantities in terms of “sums over paths”. This method is considerably different from the standard ones that have been employed so far (e.g., transforming the problem to momentum space and computing E_T numerically). In particular, it allows the analytic calculation of physical quantities as explicit functions of a continuously-tunable flux, while other approaches need to separately consider different cases (e.g., matrices) for several discrete (rational) values of the magnetic field. The lattice path approach can also be used for a variety of other physical problems, including the derivation and analysis of the superconducting transition temperature in wire networks and Josephson-junction arrays (see, e.g., Refs. 10 and 11), and the analytical

ACKNOWLEDGMENTS

We thank A. Rojo for conversations and for bringing to our attention Ref. 7, and G. Vignale for useful comments on the manuscript. We thank O. Pla, supported by NATO grant CRG-931417, for his help. We acknowledge partial support from the University of Michigan Horace H. Rackham School of Graduate Studies, and the Offices of the Vice Presidents for Research and Academic Affairs.

* Present address: Department of Physics, West Virginia University, Morgantown, West Virginia 26506-6315.

† Electronic address: nori@umich.edu

¹ See, e.g., I. Affleck and J. B. Marston, *Phys. Rev. B* **37**, 3774 (1988); Y. Hasegawa *et al.*, *Phys. Rev. Lett.* **63**, 1519 (1989); P. Lederer, D. Poilblanc, and T. M. Rice, *ibid.* **63**, 1519 (1989); D. Poilblanc, Y. Hasegawa, and T. M. Rice, *Phys. Rev. B* **41**, 1949 (1990); F. Nori, E. Abrahams, and G. T. Zimanyi, *ibid.* **41**, 7277 (1990); M. Kohmoto and Y. Hatsugai, *ibid.* **41**, 9527 (1990); F. Nori, B. Douçot, and R. Rammal, *ibid.* **44**, 7637 (1991); and references therein.

² F. Nori and Y.-L. Lin, *Phys. Rev. B* **49**, 4131 (1994).

³ E. H. Lieb, *Phys. Rev. Lett.* **73**, 2158 (1994).

⁴ P. Skudlarski and G. Vignale, *Phys. Rev. B* **43**, 5764 (1991).

⁵ Y. Hasegawa, *J. Phys. Soc. Jpn.* **59**, 4384 (1990).

⁶ Z. Kunszt and A. Zee, *Phys. Rev. B* **44**, 6842 (1991).

⁷ W. F. Brinkman and T. M. Rice, *Phys. Rev. B* **2**, 1324 (1970).

⁸ C. Kittel, *Introduction to Solid State Physics*, 6th ed. (John Wiley & Sons, New York, 1986); and N. W. Ashcroft and N. D. Mermin, *Solid State Physics* (Saunders College, Philadelphia, 1976).

⁹ R. Landauer and M. Buttiker, *Phys. Rev. Lett.* **54**, 2049 (1983).

¹⁰ Q. Niu and F. Nori, *Phys. Rev. B* **39**, 2134 (1989).

¹¹ Y.-L. Lin and F. Nori, *Phys. Rev. B* **50**, 15953 (1994).

¹² Y.-L. Lin and F. Nori, *Phys. Rev. Lett.* **76** 4580 (1996); *Phys. Rev. B* **53**, 15543 (1996).

TABLE I. Lattice path-integrals \mathcal{S}_{2l} (with the order $2l = 4, 6, 8, 10, 12$) for the 3D cubic lattice in various flux configurations: $(0, 0, \phi)$, $(0, \phi, \phi)$, (ϕ, ϕ, ϕ) , $(\phi, \phi, -2\phi)$, and the asymmetric case (π, π, ϕ) .

$2l$	\mathcal{S}_{2l} in $(0, 0, \phi)$
4	$82 + 8 \cos \phi$
6	$1452 + 384 \cos \phi + 24 \cos 2\phi$
8	$29218 + 13440 \cos \phi + 1960 \cos 2\phi + 96 \cos 3\phi + 16 \cos 4\phi$
10	$638756 + 422800 \cos \phi + 96760 \cos 2\phi + 11760 \cos 3\phi + 2284 \cos 4\phi + 160 \cos 5\phi + 40 \cos 6\phi$
12	$14865220 + 12737640 \cos \phi + 3909984 \cos 2\phi + 764216 \cos 3\phi + 182328 \cos 4\phi$ $+ 28392 \cos 5\phi + 7680 \cos 6\phi + 528 \cos 7\phi + 144 \cos 8\phi + 24 \cos 9\phi$
$2l$	\mathcal{S}_{2l} in $(0, \phi, \phi)$
4	$74 + 16 \cos \phi$
6	$1188 + 576 \cos \phi + 96 \cos 2\phi$
8	$22186 + 16736 \cos \phi + 4976 \cos 2\phi + 736 \cos 3\phi + 96 \cos 4\phi$
10	$460236 + 461760 \cos \phi + 186360 \cos 2\phi + 49760 \cos 3\phi + 11840 \cos 4\phi + 2080 \cos 5\phi + 520 \cos 6\phi$
12	$10354220 + 12623616 \cos \phi + 6211104 \cos 2\phi + 2269840 \cos 3\phi + 742800 \cos 4\phi$ $+ 209328 \cos 5\phi + 67008 \cos 6\phi + 14016 \cos 7\phi + 3744 \cos 8\phi + 480 \cos 9\phi$
$2l$	\mathcal{S}_{2l} in (ϕ, ϕ, ϕ)
4	$66 + 24 \cos \phi$
6	$948 + 756 \cos \phi + 144 \cos 2\phi + 12 \cos 3\phi$
8	$16626 + 19392 \cos \phi + 6744 \cos 2\phi + 1584 \cos 3\phi + 336 \cos 4\phi + 48 \cos 5\phi$
10	$338616 + 483420 \cos \phi + 230340 \cos 2\phi + 82980 \cos 3\phi + 27000 \cos 4\phi + 7740 \cos 5\phi + 1980 \cos 6\phi + 420 \cos 7\phi + 60 \cos 8\phi$
12	$7672212 + 12250440 \cos \phi + 7095780 \cos 2\phi + 3290664 \cos 3\phi + 1370952 \cos 4\phi + 528120 \cos 5\phi + 193524 \cos 6\phi$ $+ 65736 \cos 7\phi + 20952 \cos 8\phi + 5952 \cos 9\phi + 1512 \cos 10\phi + 288 \cos 11\phi + 24 \cos 12\phi$
$2l$	\mathcal{S}_{2l} in $(\phi, \phi, -2\phi)$
4	$66 + 16 \cos \phi + 8 \cos 2\phi$
6	$912 + 528 \cos \phi + 336 \cos 2\phi + 48 \cos 3\phi + 36 \cos 4\phi$
8	$14930 + 14016 \cos \phi + 10080 \cos 2\phi + 3040 \cos 3\phi + 1992 \cos 4\phi + 384 \cos 5\phi + 240 \cos 6\phi + 32 \cos 7\phi + 16 \cos 8\phi$
10	$282796 + 356640 \cos \phi + 275560 \cos 2\phi + 122640 \cos 3\phi + 79780 \cos 4\phi + 28160 \cos 5\phi + 17280 \cos 6\phi$ $+ 5280 \cos 7\phi + 3040 \cos 8\phi + 800 \cos 9\phi + 440 \cos 10\phi + 80 \cos 11\phi + 60 \cos 12\phi$
12	$6045696 + 9120912 \cos \phi + 7393704 \cos 2\phi + 4172032 \cos 3\phi + 2809680 \cos 4\phi + 1342512 \cos 5\phi$ $+ 841808 \cos 6\phi + 367440 \cos 7\phi + 220836 \cos 8\phi + 90384 \cos 9\phi + 52800 \cos 10\phi + 19680 \cos 11\phi$ $+ 11856 \cos 12\phi + 3696 \cos 13\phi + 2112 \cos 14\phi + 576 \cos 15\phi + 360 \cos 16\phi + 48 \cos 17\phi + 24 \cos 18\phi$
$2l$	\mathcal{S}_{2l} in (π, π, ϕ)
4	$50 + 8 \cos \phi$
6	$492 + 192 \cos \phi + 24 \cos 2\phi$
8	$5410 + 3456 \cos \phi + 808 \cos 2\phi + 96 \cos 3\phi + 16 \cos 4\phi$
10	$64676 + 56720 \cos \phi + 18680 \cos 2\phi + 4080 \cos 3\phi + 1000 \cos 4\phi + 160 \cos 5\phi + 40 \cos 6\phi$
12	$826820 + 900840 \cos \phi + 372384 \cos 2\phi + 113336 \cos 3\phi + 35448 \cos 4\phi$ $+ 9192 \cos 5\phi + 2880 \cos 6\phi + 528 \cos 7\phi + 144 \cos 8\phi + 24 \cos 9\phi$

FIGURE CAPTIONS

FIG. 1. Lower frame: Total kinetic energy of electrons at half-filling $E_T(\phi)$ for the 3D cubic lattice for various flux orientations: $(0, 0, \phi)$ (long dash), $(0, \phi, \phi)$ (short dash), (ϕ, ϕ, ϕ) (solid), $(\phi, \phi, -2\phi)$ (dot), and (π, π, ϕ) (dot-dash). Upper frame: $E_T^{(2D)}(\phi)$ for the 2D square lattice in a perpendicular field. The flux values where the minima occur are indicated. We obtain these results by using the lattice path-integrals up to the order 40 for the 3D case and 76 for the 2D lattice—which corresponds to summing contributions over $\sim 10^{29}$ electron closed paths in a 3D cubic lattice and $\sim 10^{44}$ electron closed paths in a 2D square lattice. Notice that $E_T(\phi)$ has the absolute minimum at $\phi/2\pi = 1/2$ for all of these flux orientations, except for the configuration $(0, 0, \phi)$.

FIG. 2. Total kinetic energy of electrons at half-filling E_T for the 3D cubic lattice for various field orientations: $(1/2, 1/2, 1/2)$, $(1/3, 1/3, 1/3)$, $(1/4, 1/4, 1/4)$, $(0, 1/2, 1/2)$, $(0, 1/3, 1/3)$, $(0, 1/4, 1/4)$, $(0, 0, 1/2)$, $(0, 0, 1/3)$, and $(0, 0, 0)$. Here (a, b, c) means that the three fluxes through the elementary plaquettes on the yz -, zx - and xy -planes are respectively $a/2\pi$, $b/2\pi$ and $c/2\pi$. The horizontal axis ($2L$) denotes the order of the highest-order lattice path-integral used in computing E_T . The dashed lines indicate the corresponding values from Ref. 5, where only the first three significant figures are available, except for the cases $(1/2, 1/2, 1/2)$ and $(0, 0, 0)$. The E_T reach steady values which are consistent, within $\sim 2\%$, with numerical ones for lattice path-integrals of order $2L$ equal to either 4, 6, or 8, depending on the field orientation. Higher order lattice path-integrals provide negligible contributions to E_T . Notice that the vertical axes here cover very narrow range of values ($\sim 10^{-2}$). For $(1/2, 1/2, 1/2)$, $(0, 1/2, 1/2)$ and $(0, 0, 1/2)$, both approaches give the same result within $\sim 1\%$ for $2L \geq 8$ and within $\sim 2\%$ for $2L \geq 8, 8,$ and $4,$ respectively. For $(1/3, 1/3, 1/3)$, $(0, 1/3, 1/3)$ and $(0, 0, 1/3)$, both approaches provide the same result within $\sim 1\%$ for $2L \geq 12, 10,$ and $12,$ and within $\sim 2\%$ for $2L \geq 8, 4,$ and $4,$ respectively. For $(1/4, 1/4, 1/4)$, $(0, 1/4, 1/4)$ and $(0, 0, 0)$, both approaches yield the same result within $\sim 1\%$ for $2L \geq 16, 4, 4$ and within $\sim 2\%$ for $2L \geq 4, 4,$ and $4,$ respectively.

FIG. 3. The negative of the zero-field susceptibility $-\chi(\mu)$ as a function of the Fermi energy μ for various flux configurations: $(0, 0, \phi)$, $(0, \phi, \phi)$, (ϕ, ϕ, ϕ) , and $(\phi, \phi, -2\phi)$ corresponding to curves a , b , c , and d , respectively. Curve a is always the closest to the dotted reference line $\chi = 0$, while curve d is always the farthest from it. For all these orientations, the susceptibility exhibits a very non-monotonic behavior. For small electron filling ν (i.e., small μ), diamagnetism ($\chi < 0$) dominates in spite of small fluctuations of $-\chi$ around zero. With increasing μ , on the average, $-\chi$ decreases from a large positive value to a negative one. For $\mu \geq -3.2$ the orbital response is paramagnetic.

FIG. 4. The negatives of the magnetic moment $-M(\phi)$ (left column) and the orbital susceptibility $-\chi(\phi)$ (right column) at half-filling as a function of the flux ϕ for various flux orientations as indicated. From top to bottom they are: $(0, 0, \phi)$, $(0, \phi, \phi)$, (ϕ, ϕ, ϕ) , and $(\phi, \phi, -2\phi)$. Both $-M$ and $-\chi$ exhibit non-periodic oscillations. Notice the change of the amplitude and the frequency of the oscillations as a function of the flux for different orientations of the field. At $\phi = 0$ and π , the magnetic moments are always zero. Moreover, paramagnetism exists at $\phi = 0$ for all these flux orientations. However, when $\phi/2\pi = 1/2$, the magnetic response is paramagnetic for flux configuration $(0, 0, \phi)$, and diamagnetic for the other three orientations.

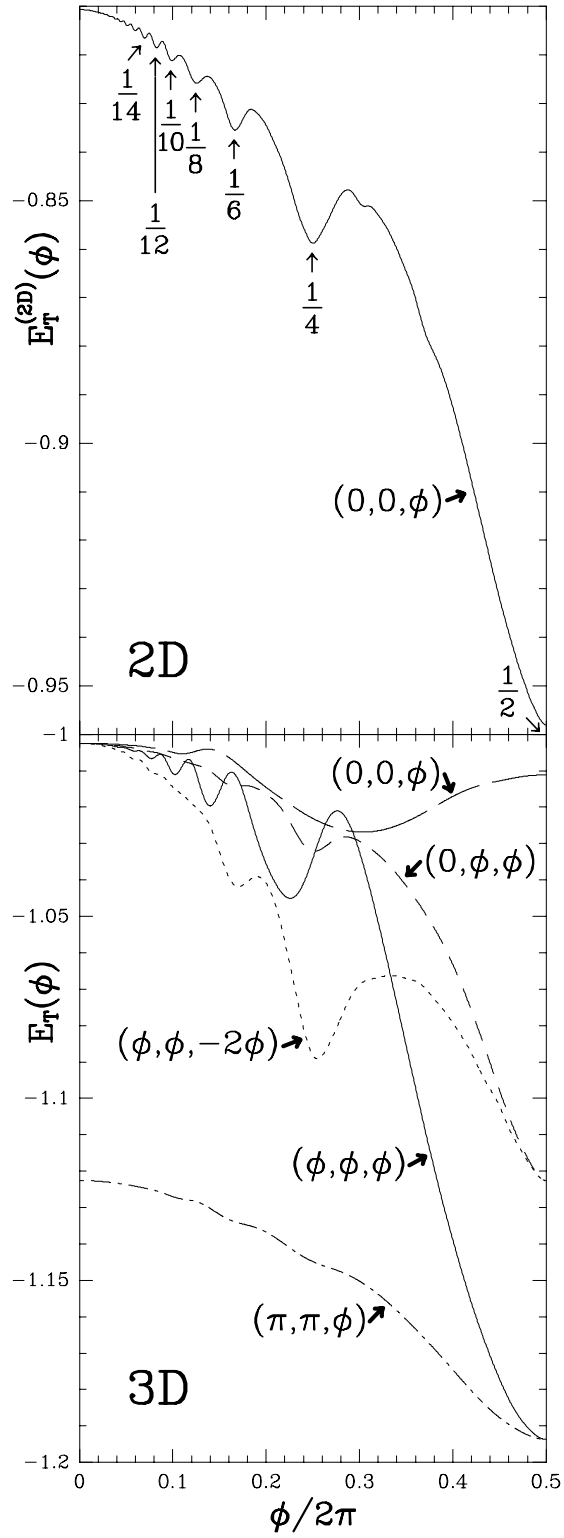


FIG. 1

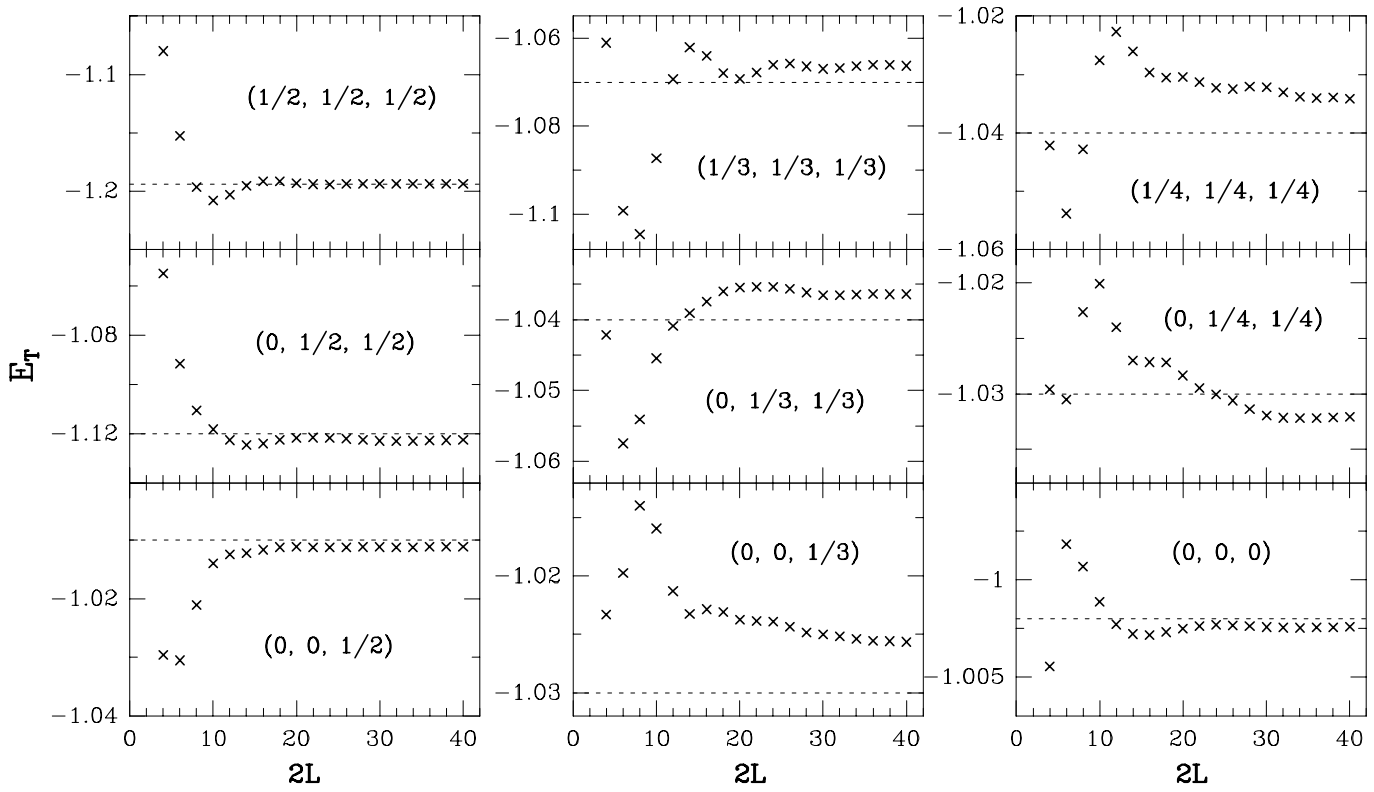


FIG.2

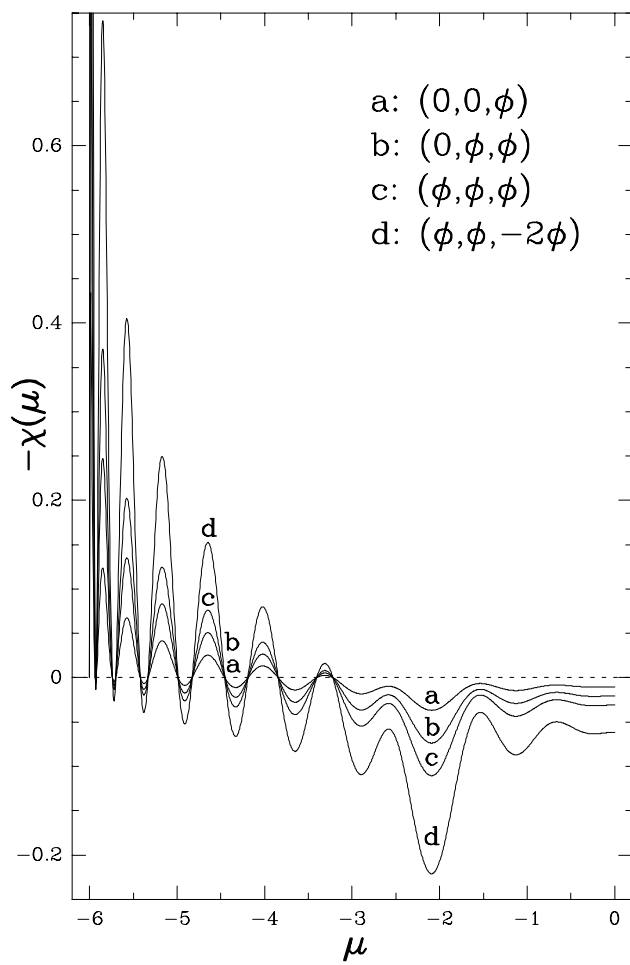


FIG. 3

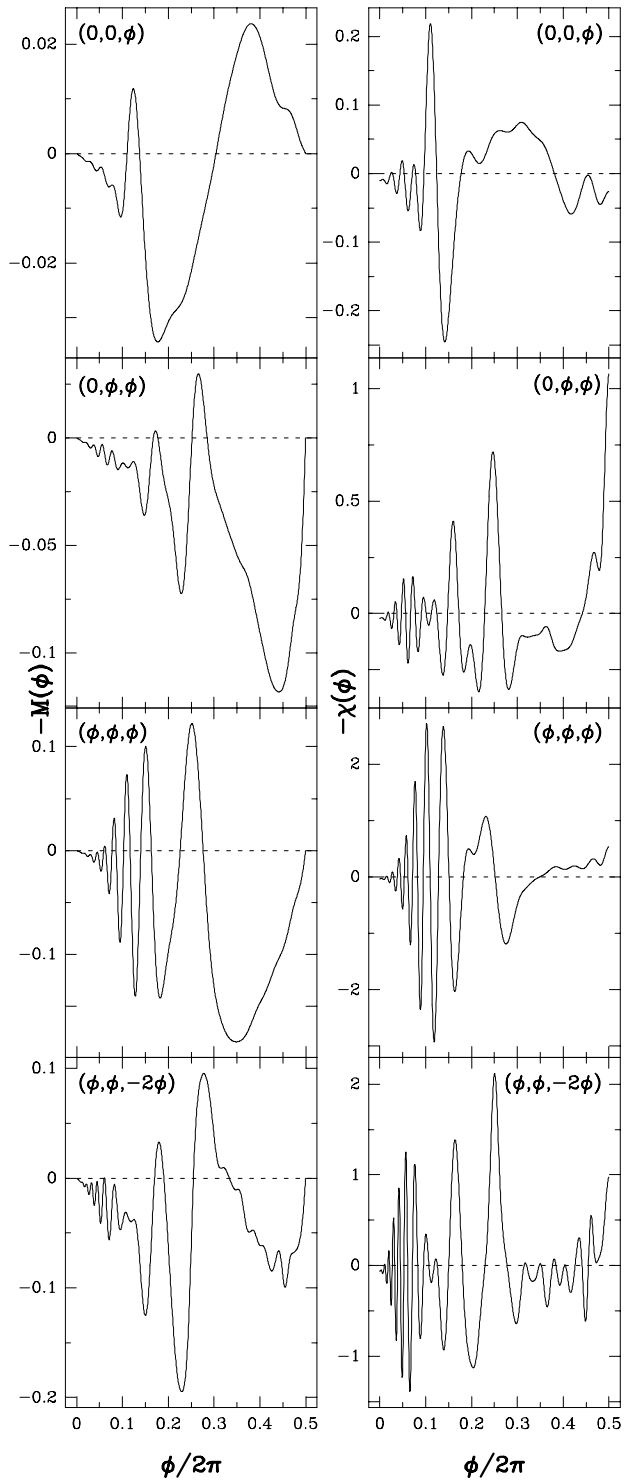


FIG. 4